Probing the ladder spectrum arising from motion in a 2-D lattice driven by an in-plane constant force

W. Yan^{1,2}, F. Claro¹, Z.Y. Zeng¹, Y.L. Zhao² and J.Q. Liang²

¹Facultad de Física, Pontificia Universidad de Católica de Chile, Casilla 306, Santiago 22, Chile

²Institute of Theoretical Physics, Shanxi University, Taiyuan, 030006, People's Republic of China

Abstract

The coherent interband dynamics of optically excited two-dimensional lateral surface superlattices driven by an in-plane static electric field has been investigated. The linear absorption, the spectrally-resolved pump-probe four-wave mixing signals and spatial coherent wavepacket evolution in the time-domain are obtained. When the rational condition $E_x/E_y = p/q$, with p,q prime to each other, is fullfilled, it is found that p peaks appear within the frequency interval $\omega_{Bx} = eE_x a/\hbar$ in both linear absorption and degenerate four-wave mixing signals. The coherent time evolution of the electron-hole pair wavepacket is that of a breathing mode, with the period $2\pi p/\omega_{Bx}$, These findings are consistent with the recent spectral results (Phys. Rev. Lett. 86, 3116), hence providing a method for probing the coherent dynamics of quantum particles in 2D lattices.

PACS numbers: 78.47.+p, 73.50.Fq, 73.20.Dx

I. INTRODUCTION

Recently, there have been much investigation on the electronic and transport properties of semiconductor superlattices driven by the external static and/or time-dependent electric fields [1–14]. It is foreseen that these explorations will uncover rich physics and even find potential applications in electro-optic devices. In this context, a lot of interesting theoretical and experimental findings have been reported. Among these, we mention Bloch oscillations [1], Fano resonances [5], absolute negative conductivity [6], inverse Bloch oscillators [7], dynamic localization [6,8], dynamic Franz-Keldysh effect [9], self-induced Shapiro effect [10], dynamic fractional Wannier-Stark ladders [11]. Particularly, with the development of atom optics, physicists began to link solid state physics and optics together, both theoretically and experimentally [15]. The recent clean demonstration of Wannier-Stark ladders [16] and Bloch oscillations [17] in the atom optics are typical examples.

Several months ago, Glück et al calculated numerically the ground Wannier-Bloch band of a quantum particle moving in a lattice under an in-plane electric field [18], The lattice may be an array of quantum dots for electrons, or an interference pattern of light waves for cold atoms [15]. They found that the energy spectrum resembles the Hofstader butterfly [19] in a magnetic system, and the 1-D superlattice driven by dc-ac electric fields [11]. They showed that for a rational static force \mathbf{F} of components in the ratio $F_x/F_y = p/q$, with p,q coprime integers, there are $s = p^2 + q^2$ identical subbands separated by the energy interval $\delta \equiv |\mathbf{F}|a/\sqrt{s}$, where a is the lattice constant. Since the lattice period in the direction of the field is $\sqrt{s}a$, this result predicts a splitting of the 1-D Stark period into s equally spaced subbands. The question arises as to whether such a spectrum is measurable.

In this paper we report our finding that this striking splitting in the spectrum can be identified in optically excited two-dimensional lateral surface superlattices driven by an inplane static electric field \mathbf{E} . Such 2-D superlattices can be prepared by embedding a square array of GaAs cylinders in a very thin $Ga_xAl_{1-x}As$ epilayer [20]. By numerically solving the generalized semiconductor Bloch equations, this spectrum is identified in both the linear

absorption signal and spectrally resolved pump-probe degenerate four-wave mixing signals. Also, we link the breathing-mode period of spatial coherent wavepackets oscillations in the time domain in the system to the splitting of the spectrum.

II. MODEL AND NUMERICAL RESULTS

We consider an electron system moving in a 2-D lattice and an external in-plane electric field \mathbf{E} with its component in the ratio $E_x/E_y=p/q$, where p and q are coprime numbers. The energy dispersion is treated in a two-band model, the valence and conduction bands. We discuss the dynamics in the context of the following semiconductor Bloch equations [2-4,22]

$$\left(\frac{\partial}{\partial t} + \frac{e}{\hbar} \mathbf{E}(t) \cdot \nabla_{\mathbf{k}}\right) P_{\mathbf{k}}(t) = -\frac{i}{\hbar} [e_{e,\mathbf{k}} + e_{h,\mathbf{k}} - i\Gamma_L] P_{\mathbf{k}}(t) - \frac{i}{\hbar} [n_{e,\mathbf{k}} + n_{h,\mathbf{k}} - 1] \omega_{R,\mathbf{k}} \tag{1}$$

$$\left(\frac{\partial}{\partial t} \pm \frac{e}{\hbar} \mathbf{E}(t) \cdot \nabla_{\mathbf{k}}\right) n_{e(h)\mathbf{k}}(t) = -2 \text{Im}[\omega_{R,\mathbf{k}} P_{\mathbf{k}}^*] - \Gamma_T n_{e,(h)\mathbf{k}}(t), \tag{2}$$

where $P_{\mathbf{k}}(t)$ is the interband polarization and $n_{e(h),\mathbf{k}}(t)$ the electron (hole) population density in the conduction (valence) band. The quantities $e_{i,\mathbf{k}} = \epsilon_{i,\mathbf{k}} - \sum_{\mathbf{q}} V_{|\mathbf{k}-\mathbf{q}|} n_{i,\mathbf{q}}$, (i=e,h)are the renormalized electron and hole energies due to the Coulomb interaction. Also, $\omega_{R,\mathbf{k}} = (d_{cv}\mathcal{E} + \sum_{\mathbf{k}} V_{|\mathbf{k}-\mathbf{q}|} P_{\mathbf{q}})/\hbar$ are the renormalized Rabi frequencies, with d_{cv} the dipole moment and $\mathcal{E}(t)$, the Gaussian laser pulses. The relaxation time approximation has been assumed, with Γ_L and Γ_T being the longitudinal and transverse relaxation rates, respectively.

The spectrally-resolved absorption, pump-probe nonlinear four-wave mixing signals and the real-time coherent evolution of the wavepackets in real-space have been calculated numerically by solving the coupled Eqs.(1) and (2). The energy bands of 2-D lateral surface superlattices of square geometry can be described by the tight-binding form [20,21,23] $\epsilon_i(\mathbf{k}) = \frac{\Delta_i}{2}(\cos(k_x a) + \cos(k_y a))$ (i = e, h), with $\Delta_c(\Delta_v)$ being the combined miniband width

of the conduction (valence) band in the x and y directions. For simplicity, an on-site Coulomb interaction has been adopted, which describes the first-order Born scattering among the carriers. Although the excitonic interaction is simplified to be on-site in this work, it is expected that the inclusion of more realistic models will not change our findings qualitatively. This kind of approximation has been used with success by many groups [2-4,13,24].

Linear absorption: In the linear response regime, one can completely neglect Eq.(2), and set the electron (hole) density $n_{c(v)}(\mathbf{k},t)$ to vanish in Eq. (1). The absorption $\alpha(\omega)$ is proportional to the imaginary part of the first-order susceptibility $\chi^{(1)}(\omega) = \text{Im}[P^{(1)}(\omega)/E(\omega)],$ where $P^{(1)}(\omega)$ is the Fourier transform of the quantity $\sum_{\mathbf{k}} P^{(1)}(\mathbf{k}, t)$. The integro-differential equations can be solved numerically in the accelerated basis $\mathbf{k} - \frac{e}{\hbar} \int_0^t \mathbf{E}(\tau) d\tau$. Parameter values used in the calculations are $\Delta_c = \Delta_v = 20$ meV, V = 10 meV, and $\Gamma_L = \Gamma_T = 0.5$ THz. The full width at half maximum for the strength of the Gaussian laser pulse is assumed to be 59 femtoseconds. In the simulation the Bloch frequency $\omega_{Bx} = eE_x a/\hbar$ of the static electric field in the x direction remains unchanged and taken to be 3π THz, while the Bloch frequency $\omega_{By} = eE_y/\hbar$ in the y direction takes three different values: $1/3 \omega_{Bx}$, $2/3 \omega_{Bx}$, and $4/3 \omega_{Bx}$. Distinct peaks are clearly identified in the three panels, where the ratio E_x/E_y is indicated in the right-up corner. Roughly three peaks appear within every interval ω_{Bx} in the three panels, although the Bloch frequencies in the y direction differ by a factor of four in the top and bottom panels. This property is the direct reflection of the striking spectrum discussed by Glück et al [18]. Since $\omega_{Bx} = eE_x a/\hbar \equiv (p|e\mathbf{E}|/\sqrt{s})(a/\hbar)$, and the characteristic energy splitting $\delta = |e\mathbf{E}|a/\hbar\sqrt{s}$, then $\delta/\omega_{Bx} = 1/p$, where for Fig.1, p=3 in all three panels. The interesting and special case of $E_x:E_y=3:3=1:1$ is shown in the Fig.2, where peaks appear only once in the fixed interval ω_{Bx} . It is clear from the comparison of Fig.1 and Fig.2 that the number of peaks appearing in the fixed frequency interval ω_{Bx} is solely determined by the integer p, instead of the absolute value of E_x and E_{y} . It should be noted that the absorption peaks obtained in the present model are much more stable that those in dc-ac field case [25]. The latter are easily blurred by the dephasing and Coulomb interaction-mediated Fano interferences [5].

Four-wave mixing signals: Four-wave mixing experiments are usually applied to observe the coherent signals from optically excited semiconductor samples by taking advantage of the fact that this technique can substantially avoid the inhomogeneous broadening [2]. In order to mimic the experimental realization of probing the spectrum, the two laser pulses: the strong pump pulse propagating in the \mathbf{k}_1 direction, and the weak probe pulse propagating in the direction \mathbf{k}_2 , are arranged to be delayed a time τ_p relative to each other,

$$\mathcal{E}(t) = \mathcal{E}_1(t) \exp[i(\mathbf{k}_1 \cdot \mathbf{r} - \omega t)] + \mathcal{E}_2(t - \tau_p) \exp[i(\mathbf{k}_2 \cdot \mathbf{r} - \omega (t - \tau_p))].$$
(3)

One can use the method of Lindberg et al [26], or that by Banyai et al [27], to extract the nonlinear pump-probe four-wave mixing signals propagating in the direction $2\mathbf{k}_2 - \mathbf{k}_1$. The spectrally-resolved pump-probe degenerate four-wave mixing squared signals are shown in the four panels of Fig.3 for different values of τ_p . A Gaussian profile for the pump and probe laser fields $\mathcal{E}_1(t)$ and $\mathcal{E}_2(t)$ is assumed, and the other parameters used are the same as those in Fig.1. In the figure, we only show the case of $\omega_{By}/\omega_{Bx} = 2/3$. The other sample cases $\omega_{By}/\omega_{Bx} = 1/3, 4/3$ have similar shape, and are omitted for saving space. Inspection of the four panels clearly show that the peaks also appear three times in the frequency interval ω_{Bx} , although a different time delay τ_p is employed in different panels. This demonstrates that there exists the energy interval/ladders in the system whose energy spacing is identical and equal to $\omega_{Bx}/3$. This is a direct manifestation of the split stable resonance spectrum found in 2-D lattices under an external in plane uniform field.

Coherent wavepacket oscillations: As is well known, the time-domain wavepacket Bloch oscillations inferred from the semiclassical approach are a direct proof of the frequency-domain resonance states of Wannier-Stark ladders [1]. While in Fig.1-3 the signals are all from the frequency domains, what about the evolution of the coherent wavepacket in the time and spatial domain? In the following, we will show the coherent spatial wavepacket oscillatory behavior in the realm-time domain [30].

According to the definition of the electron-hole wavepackets [29]: $P(\mathbf{r},t) = |\sum_{\mathbf{k}} \exp(-i\mathbf{k}\cdot$

 \mathbf{r}) $P_{\mathbf{k}}(t)$ |², where \mathbf{r} is the relative position vector of the electron-hole pair. The coherent spatial wavepackets have been shown sequentially in Fig.4, with the corresponding time displayed in the upper-right corners. In the simulation we used the following parameters: $\omega_{Bx} = 6\pi$ THz, $E_y/E_x = 2/3$, while the other parameters used are the same as those in Fig.1. The contour of the wavepacket in the earliest time (t = 0.05 ps) looks like a small circular dot, which can be regarded as the profile of the initial excitation of the electronhole pair. With the development of time (t = 0.20 ps), due to the driving electric field, the wavepacket is pulled apart and distributed along both the x and y directions in a anisotropic manner. When time reaches 0.5 ps, the wavepacket distribution along the y direction is reduced. This is expected because the Bloch oscillations period along the y direction is $T_{By} = 2\pi/\omega_{Bx} = 0.5$ ps. For the same reason, the wavepacket distribution experiences narrowing along the direction x at time $t = 0.67 \ ps (\approx 2T_{Bx})$. At time $t = 0.8 \ ps$, the wavepacket again inflates in both x and y directions. The most striking phenomena perhaps lies in the last panel, where the wavepacket has shrunk into a small constellate at time t=1ps. Since $T = 2\pi\hbar/\delta = 2\pi p/\omega_{Bx}$, for the frequency chosen one obtains T = 1 ps, which equals three times T_{Bx} , and twice T_{By} . This indicates that the energy splitting δ found in Ref. [18] is the direct consequence of the wavepacket Bloch oscillations with period T of the electron-hole pair, although no hole motions are involved in Ref. [18]. The existence of this period is thus a direct manifestation of *commensurate* synchronous Bloch oscillations in both x and y directions. It should be mentioned in passing that in the absence of excitonic interaction, the wavepacket will undergo the breathing mode in a precise time period T. The presence of the interaction changes only slightly this period.

III. CONCLUDING REMARKS

The linear absorption and nonlinear pump-probe spectrally resolved four-wave mixing signals have been calculated in optically excited 2-D lateral surface superlattices driven by an in-plane static electric field. The ratio of E_x to E_y is chosen to be the rational p/q,

making the peaks appear p times in the frequency interval ω_{Bx} , both in linear absorption and the four-wave mixing signal. This finding provides a way to test experimentally the spectrum arising in the dynamics of particles moving in a 2D lattice and a constant force [18]. Also the coherent wavepacket oscillates with a period corresponding exactly to that associated with the energy interval δ , showing that the energy interval is a consequence of the commensurate synchronous Bloch oscillations in both the x and y directions.

Theoretically, in the absence of all kinds of dephasing [18], the spectrum has the property of extreme sensitivity to fluctuations in the direction of the field. For instance, if $E_y/E_x = q/p$, then an arbitrarily small rotation yields a ratio q'/p', with $(q', p') \to \infty$. For instance, if q/p = 1/3, a tiny change in the field produces the fraction 1001/3000, while an even smaller change gives rise to the ratio 1000001/3000001, thus modifying wildly the splitting size as determined by the denominator fraction. The presence of various kinds of dephasing mechanisms blur this fine structure, making the identification of the peak in the fixed interval ω_{Bx} impossible, when p becomes large [31]. Experimentally, the phenomena predicted here can be observed in a photoexcited 2D quantum dot array driven by an in-plane electric field, with the electric field strength tuned to be a rational. It is expected that *clean* observation of these ladders can be also realized in ultracold atoms dwelling in the two perpendicular optical waves, accelerated accordingly.

ACKNOWLEDGMENT

This work was supported in part by Cátedra Presidencial en Ciencias (F.C.) and FONDE-CYT, Grants 1990425 and 3980014; W.Y. is supported in part by the Youth Science Foundation of Shanxi Province of PRC.

REFERENCES

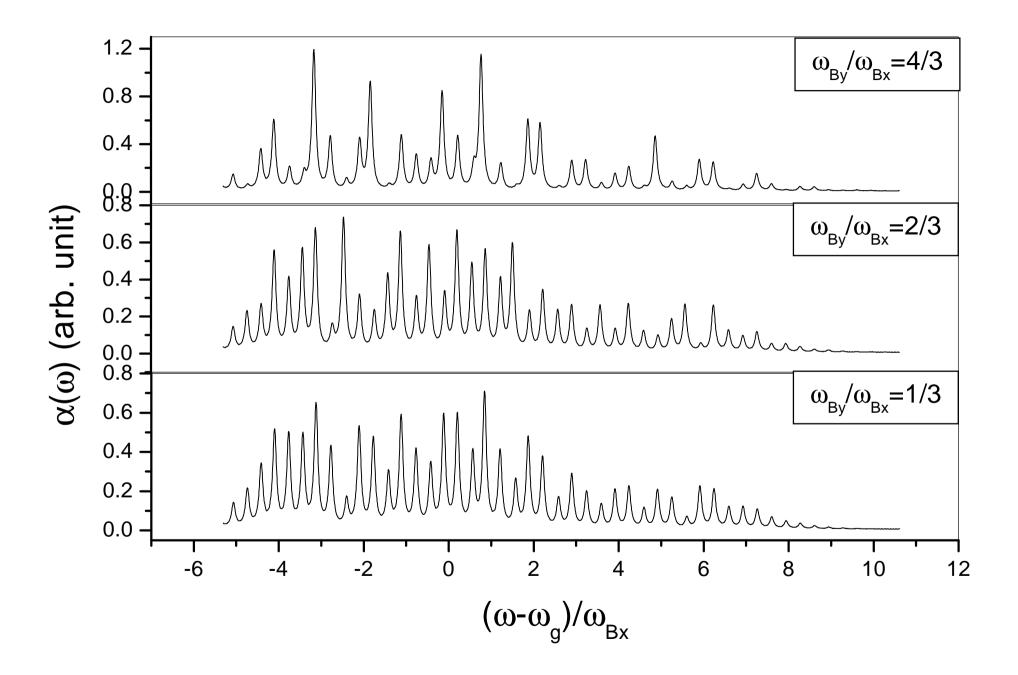
- [1] E.E. Mendez and G. Bastard, Phys. Today, 50, No.7, 30 (1993) and references therein.
- [2] T. Meier, G. von Plessen, P. Thomas, S.W. Koch, Phys. Rev. Lett. 73, 902 (1994);Phys. Rev. B 51, 14490 (1995).
- [3] T. Meier, F. Rossi, P. Thomas, and S.W. Koch, Phys. Rev. Lett. **75**, 2558 (1995).
- [4] V.M. Axt, G. Bartels, and A. Stahl, Phys. Rev. Lett. **76**, 2543 (1996).
- [5] For Fano resonance in superlattices driven by dc field, see D.M. Whitakker, Europhys. Lett. 31, 55 (1995); Norbert Linder, Phys. Rev. B 55, 13664 (1997); C.P. Holfeld, F. Löser, M. Sudzius, K. Leo, D.M. Whitakker, and K. Köhler, Phys. Rev. Lett. 81, 874 (1998); S. Glutsch, and F. Bechstedt, Phys. Rev. B 60, 16584 (1999); for dc-ac Fano resonance case, see R.-B. Liu and B.-F. Zhu, J. Phys. Conden. Matter, 12, L741 (2000).
- [6] B.J. Keay, S. Zeuner, S.J. Allen, K.D. Maranowski, A.C. Gossard, U. Bhattacharya, and M.J.W. Rodwell, Phys. Rev. Lett. 75, 4102 (1995).
- [7] K. Unterrainer, B.J. Keay, M.C. Wanke, S.J. Allen, D. Leonard, G. Medeiros-Ribeiro, U. Bhattacharya, and M.J.W. Rodwell, Phys. Rev. Lett. 76, 2973 (1996).
- [8] D.H. Dunlap, and V.M. Kenkre, Phys. Rev. B **34**, 3625 (1986).
- [9] A.P. Jauho, and K. Johnsen, Phys. Rev. Lett. **76**, 4576 (1996).
- [10] F. Löser, M.M. Dignam, Yu. A. Kosevich, K. Köhler, and K. Leo, Phys. Rev. Lett. 85, 4763 (2000).
- [11] X.-G. Zhao, R. Jahnke, and Q. Niu, Phys. Lett. A 202, 297 (1995); K.W. Madison,M.C. Fischer, and M.G. Raizen, Phys. Rev. A 60, R1767 (1999).
- [12] M. Dignam, Phys. Rev. B **59**, 5770 (1999).
- [13] R.-B. Liu and B.-F. Zhu, Phys. Rev. B **59**, 5759 (1999).

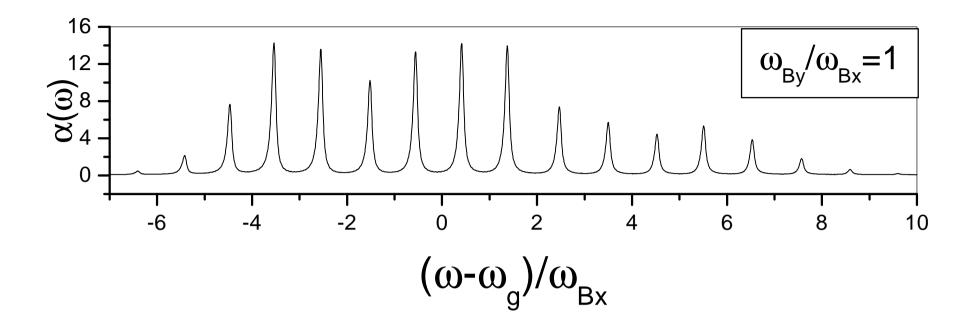
- [14] J. Hader, T. Meier, S.W. Koch, F. Rossi und N. Linder, Phys. Rev. B. 55, 13799 (1997).
- [15] M. Raizen, C. Salomon, and Q. Niu Phys. Today, **50** No.7, 30 (1997)
- [16] For experiment see, S.R. Wilkinson, C.F. Bharucha, K.W. Madison; for theoretical interpretation, see Q. Niu, and M.G. Raizen, Phys. Rev. Lett. 76, 4512; Q. Niu, X.-G. Zhao, G.A. Georgakis, and M.G. Raizen, *ibid.* 76, 4504.
- [17] M.B. Dahan, E. Peik, J, Reichel, Y. Castin, and C. Salomon, Phys. Rev. Lett. 76, 4508.
- [18] M. Glück, F. Keck, A.R. Kolovsky, and H.J. Korsch, Phys. Rev. Lett. 86, 3116 (2001).
- [19] D.R. Hofstader, Phys. Rev. B 14, 2239 (1976).
- [20] R.K. Reich, R.O. Grondin, and D.K. Ferry, Phys. Rev. B 27, 3483 (1983).
- [21] A.P. Silin, Sov. Phys. USP. 28, 972 (1985). (Usp. Fiz. Nauk, 147, 485-521 (1985)).
- [22] M. Lindberg, and S.W. Koch, Phys. Rev. B 38, 3342 (1988); for a systematic review, see H. Haug, and S.W. Koch, Quantum theory of the optical and electronic properties of semiconductors, 3rd. Ed. (World Scientific, Singapore), (1994) and references therein.
- [23] J.H. Davies, and J.W. Wilkins, Phys. Rev. B 38, 1667 (1988).
- [24] W. Yan, X.-G. Zhao, and H. Wang, J. Phys.: Conden. Matter 10, L11 (1998); W. Yan,
 S.-Q. Bao, X.-G. Zhao, and J. Q. Liang, Phys. Rev. B 61, 7269 (2000).
- [25] W. Yan, F. Claro, Z.Y. Zeng, and J.Q. Liang, J. Phys.: Conden. Matter 13, 5103 (2001).
- [26] M. Lindberg, R. Binder, S.W. Koch, Phys. Rev. A 45, 1865 (1992).
- [27] L. Banyai, D.B. Tran Thoai, E. Reitsamer, H. Haug, D. Steinbach, U. Wehner, M. Wegner, T. Marschner, and W. Stolz, Phys. Rev. Lett. 75, 2188 (1995).
- [28] For the wavepackets in the semiconductor superlattices driven by the one-dimensional electric field, see M. Dignam, J.E. Sipe, and J. Shah, Phys. Rev. B 49, 10502 (1994).

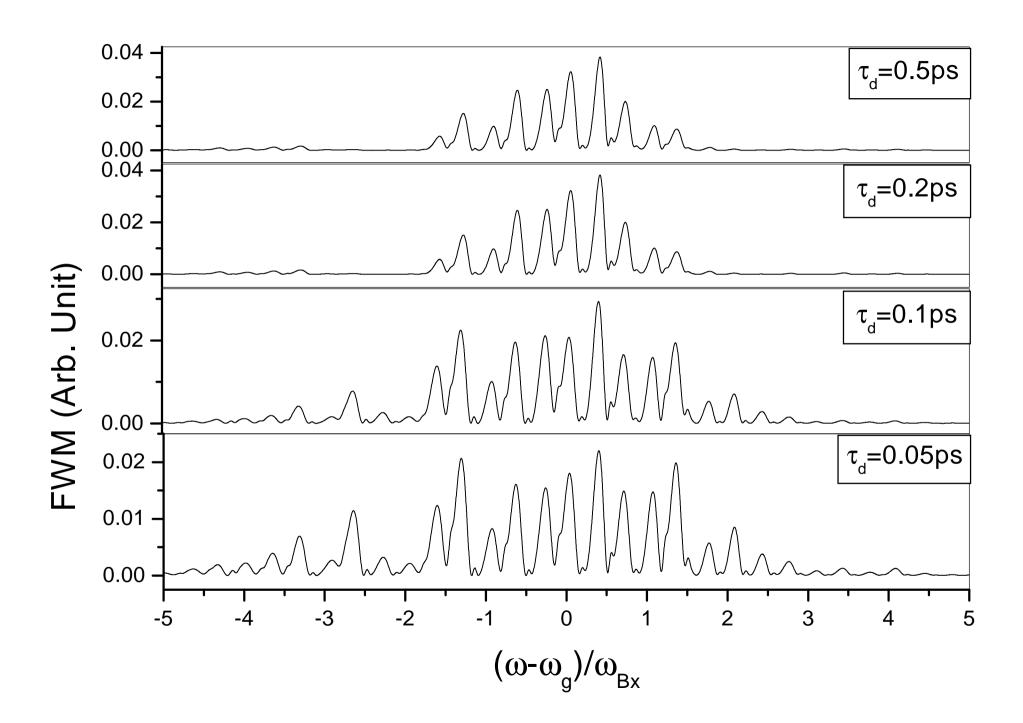
- [29] S. Hughes, and D.S. Citrin, Phys. Rev. B 59, R5288 (1999); S. Hughes, and D.S. Citrin,J. Opt. Soc. Am B 17, 128 (2000).
- [30] In order for the comparison of the Coherent wavepackets at different time t, the longitudinal and transverse depahsing rates Γ_L , Γ_T were assumed to be vanishing.
- [31] We also calculated the case of p:q=8:3, where eight clear-cut peaks appear in the frequency interval ω_{Bx} .

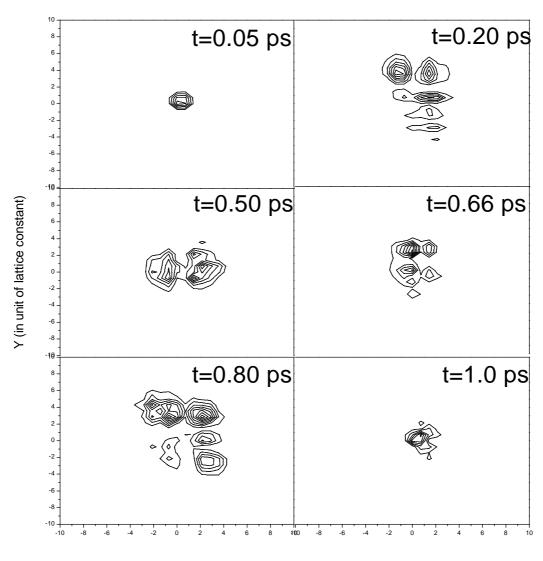
FIGURES

- FIG. 1. Linear absorption $\alpha(\omega)$ plotted as a function of $(\omega \omega_g)/\omega_{Bx}$, where ω_g is the frequency associated with the conduction-valence band gap.
- FIG. 2. The same as Fig.2, except that $\omega_{By}: \omega_{Bx} = 3:3=1:1$. Only one peak appears in every fixed frequency interval ω_{bx} .
- FIG. 3. Spectrally-resolved degenerate squared four-wave mixing signal $|P^{(3)}(\omega)|^2$ plotted as a function of $(\omega \omega_g)/\omega_{B,x}$. Three equidistant peaks appear within the fixed frequency interval ω_{Bx} .
- FIG. 4. Coherent time-evolution of a wavepacket, showing the breathing behavior in the real-time domain. The oscillatory period is 1 ps, revealing the energy spacing in the frequency/energy domain.









X (in unit of lattice constant)